Journal of Engineering Science and Technology
Vol. 14, No. 2 (2019) 1055 - 1070

PERFORMANCE EVALUATION OF SINGLE PHASE ELECTRIC WATER PUMP OPERATED AS TURBINE-GENERATOR SET

WIDODO P. M.*, RINALDY D.

Electrical Engineering Department, Engineering Faculty,
University of Indonesia, Depok, Indonesia
*Corresponding Author: widodopm@yahoo.com

Abstract

There are three problems in the use of a single-phase electric water pump as a turbine generator at an off-grid pico-hydropower plant: the pump does not have a mechanical speed regulator, the dynamic model for the reverse operation mode is unavailable, and the presence of cross-coupling effect between the voltage and frequency loop. The speed control problem was solved by applying the Electrically Balanced Load method, the dynamic model problem was solved by the data-driven estimation method, and the cross-coupling effect problem was overcome by adding decoupling blocks to the input of the plant model. All three solutions are implemented in a compact frequency voltage control design that uses dual PID controllers, as well as additional double decoupling blocks. By choosing the right values of *Kp*, *Ti*, and *Td*, the output voltage and output frequency can be produced which meet the permitted standard. It can be concluded that a small single-phase electric water pump used in this study can be used as a turbine generator for standalone pico hydroelectric power generation.

Keywords: Decoupling circuit, Double PID controller, Single-phase induction generator, Small single-phase electric water pump.

1. Introduction

People living in mountainous areas generally get clean water supply directly from the water springs. Normally, the water is distributed using long distance PVC pipes. If the altitude difference between the end pipe and the water source is high, then the water pressure at the end of the pipe will also be high. This condition may cause damage of the pipe, especially during the closing of the valve. To overcome this problem, the pipelines should not be equipped with a valve. Usually, water is flowed directly to the tank all the time, wasting the energy contained in the flow of water. This wasted energy can actually be converted into electrical energy.

This study proposed a small electric water pumps to be used as a turbine-generator set of a standalone Pico hydroelectric power generation. Since the system is assumed to be operated standalone (off-grid) in rural areas, the system must be equipped with the appropriate voltage and frequency regulator mechanisms to maintain the stable operation of the generator voltage and frequency. Considering that power generation is designed primarily for poor rural areas and located far from urban areas, the technology used must meet the following criteria; simple, easy to install by local personnel, the spare-parts should be available in the local market and low price [1].

According to Jain and Patel [2], a study on the operation of Pumps Operated as Turbine (PAT) had been conducted since 1931. Jain and Patel [2] and Motwani et al. [3] explained that the first study was done by Thoma, while the objective of his research was to study the characteristic of the centrifugal pumps operated as a turbine.

In this research, a small size single-phase electric pump was used as the object of the research. The advantage of using a small electric pump as a turbine is its simplicity in the procurement process; its low price due to mass production; and the availability of spare-parts on the free market all over the world [4-7]. In addition to the above reasons, the use of small size electric pumps is intended to develop independently power plants in every home, so there will be no expensive cost to build and maintain transmission lines or distribution lines anymore [8].

Pumps operated as turbines are particularly well suited for small-scale power generation systems in rural areas of developing countries which mostly have difficulties in terms of funds [9]. Pump manufacturers do not normally provide characteristic curves of their pumps working as turbines. The problem of using a PAT is the difficulty of predicting the turbine performance [4, 6].

In this study by Teuteberg [4], the turbine is used as a pump, which is not equipped with a guide vane for mechanical speed regulator, then according to Derakhshan and Nourbakhsh [5], the electrically balanced load method is proposed to control the rotor speed. In this case, the efficiency aspect is ignored on the assumption that the primary energy is using waste energy.

Mostly the prime mover of the single-phase electric pump is a single-phase induction motor. In this study, the single-phase induction electric motor of the pump is proposed to use as the generator. The utilization of single-phase induction motors as induction generators has been developed over the last two decades when people started to develop renewable energy [10]. The induction generator has advantages, such as simplicity, low cost, durability and low maintenance compared to the synchronous generator [11]. Another researcher stated that the induction

generator is the right candidate to generate an electric power for Distributed Generation system, such as in remote areas due to their robustness, the absence of rotor brushes and DC excitation, simplicity of construction, low maintenance, and also high power density (W/kg) [12, 13]. The other benefit of the induction generator is self-protected from short-circuit fault [13].

Induction generator which independently supplied load without being interconnected to the grid called as Self-Excited Induction Generator (SEIG) [14], while for Single Phase Generator called Single Phase Self Excited Induction Generator (SPSEIG). The major issue of the SEIG is the poor performance of the voltage output.

Chilipi et al. [15] and Chermiti and Khedher [16] commented that the characteristic of voltage and frequency outputs does not only depend on the rotor speed, but also on the capacitance of the excitation capacitor and the load profile. To overcome this problem, several schemes had been investigated by previous researchers, such as the usage of saturable core reactor, switched shunt capacitor, Static VAR Compensator (SVC) and Static Synchronous Compensator (STATCOM) [17, 18].

Other than voltage output, the frequency output of the induction generator must also be controlled to remain within the acceptable value. The main parameter that influences the output frequency is the rotor speed. Naturally, decreasing in turbine rotor speed occurs when the generator shaft torque is greater than the turbine shaft torque or vice versa. Thus, in case both shaft torques are equal, the shaft rotation will remain constant.

Referring to this philosophy, in order to maintain the rotor speed being constant at a certain value, it is necessary to control the generator load equal to the turbine power output. In this study, the turbine power output is assumed to be constant, because the turbine is not completed with a mechanical governor system. To keep constant rotor speed, the electric load should be maintained balanced with turbine output power.

Previous other researcher had also conducted a similar study by using a single phase electric water pump machine but only control the output voltage without control the frequency.

The objective of this study is to get simple, robust, and cost economic design of Pico hydropower generation, using single phase electric pump as a turbine-generator set which both voltage and frequency output are controlled simultaneously, as well as using data-driven method for estimating the transfer function.

2. Material and Methods

A 250-watt household single phase electric objective water pump was chosen as the object of the research. The pump is the centrifugal type operated in turbine mode. The electric motor is operated as a Single-Phase Self-Excited Induction Generator (SPSEIG). To collect the SPSEIG data it is necessary to rotate the rotor by using variable speed electric motor.

For this purpose, the pump is disassembling from the motor temporarily. The electric loads are four pieces of light-bulb; 60 W, 40 W, 20 W, and 10 W, respectively. While the electric dummy load is 100 watt light bulb. An SPC1-50

"Automatic" TRIAC controller is used to adjust the dummy load. Figure 1 shows the experimental setup for collecting the generator data.

Both stator windings of SPSEIG are connected in parallel with capacitors. Main winding is connected in parallel with fix capacitor while start winding is connected with 8 pieces' capacitors via switched relays. The usage of 8-bit combination switches achieved 256 variations of the capacitance value. This variation number is smooth enough to control the generator voltage output.

In this study, the capacitance value of capacitor at LSB position is 0.0068 uF, the 2^{nd} bit = 0.15 uF in, 3^{rd} bit = 0.33 uF, 4^{th} bit = 0.68 uF, 5^{th} bit = 1.2 uF, 6^{th} bit = 2.7 uF, 7^{th} bit = 5.6 uF and 8^{th} bit position = 10 uF.

The value of the above capacitors is calculated as needed and selected according to the standard size on the market. Figure 2 shows the basic schematic diagram of the variable excitation capacitor, while Fig. 3 shows the photograph of the equipment.

Fig. 1. Experimental setup.

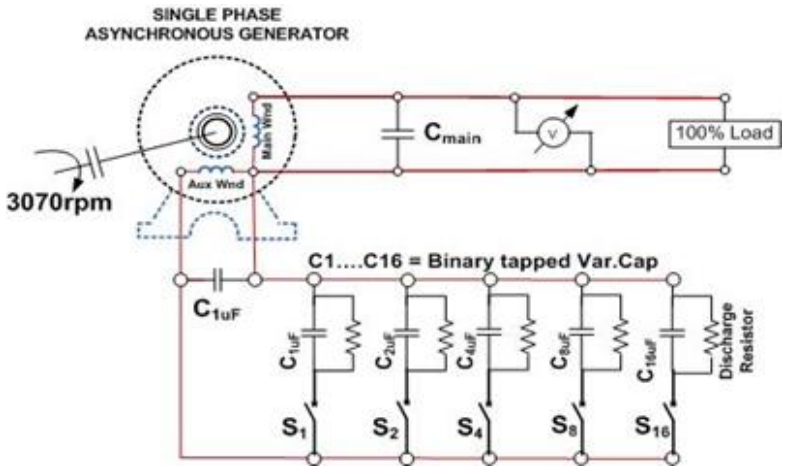

Fig. 2. Schematic diagram of binary combination switches of excitation capacitors.

Fig. 3. Binary combination switches and excitation capacitors.

2.1. Measuring the data

To conduct this study, static and dynamic parameter data of the induction generators are needed. The static parameters are; synchronous impedance (Z_{syn}), and stator resistance (R_{syn}). These two parameters are required to obtain the stator inductance winding parameter (L). The system is the MIMO system, which contains 2 inputs and 2 outputs; voltage and frequency, respectively. Four dynamic data sets are needed: data set of the dynamic response of the voltage regulator loop under open loop conditions; data set of the dynamic response of the frequency regulator path under open loop conditions; data set of the dynamic response of the cross-coupling from the voltage regulator path to the frequency regulator path; and data set of the dynamic response of the cross-coupling from the frequency regulator loop to the voltage regulator path.

Figure 4 shows the basic circuit diagram proposed for the study. The purpose of the circuit is to collect the data set to get the transfer function of the system being studied. The USB-DAQ board is used to acquire the generator voltage and frequency output, and to capture the measured data using customized DAQ software dedicated for this research.

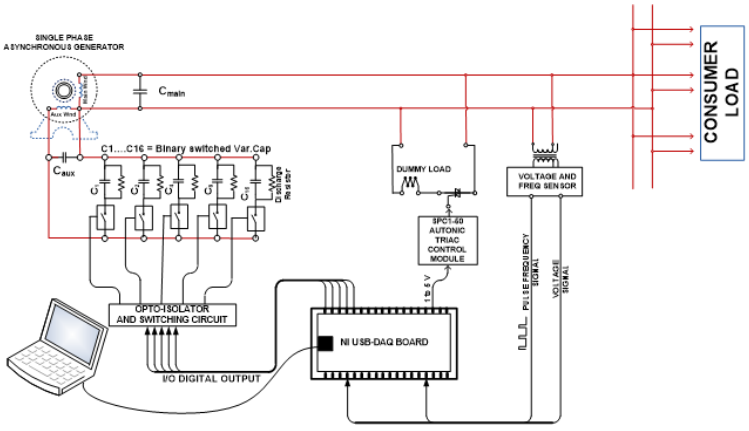

Fig. 4. Experimental schematic diagram.

2.2. Measuring synchronous inductance

Synchronous inductance is required to determine the value of the excitation capacitor connected to the main winding.

The electrical specification of the electric motor pump is shown in Table 1.

Injection of 218 volt AC in the experimental circuit diagram as shown in Fig. 5, the current flow at the main winding is 1.11 ampere, hence:

$$Z_{syn} = \frac{V_{test}}{I_{measured}} \quad (1)$$

$$Z_{syn} = \frac{218\ volt}{1.11\ Amp} = 196.39\ \text{Ohm}$$

$$X_{syn} = \sqrt{Z_{syn}^2 - R_{syn}^2} \quad (2)$$

$$X_{syn} = 2.\pi.F.L \quad (3)$$

Then,

$$L = \frac{X_{syn}}{2.\pi.F.} \quad (4)$$

where:

Z_{syn} = Synchronous Impedance (Ohm)
X_{syn} = Synchronous Reactance (Ohm)
R_{syn} =DC Resistance.(Ohm)
F = Frequency (hertz)

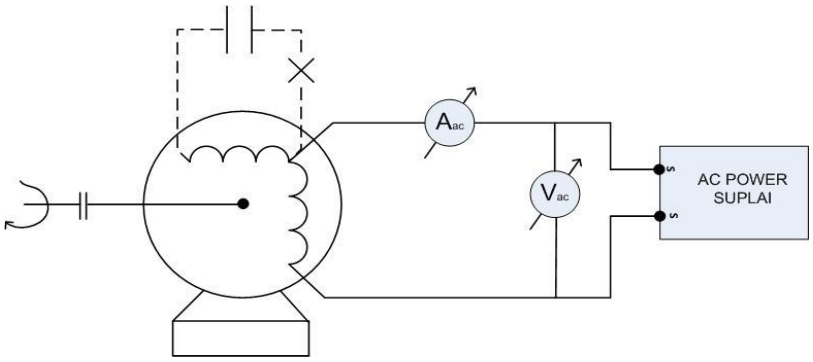

Fig. 5. Synchronous impedance measuring circuit.

The measured DC resistance of the winding by using experiment circuit diagram Fig. 6, obtained the resistance value (R) is 142.31 Ohm, hence the synchronous inductance is:

$$X_{syn} = \sqrt{196.39^2 - 142.31^2} = 135.349\ Ohm$$

$$L = \frac{X_{syn}}{2.\pi.F.} = 431.04\ mH$$

In case under-damped *LC* circuit:

$$\omega_o = 2.\pi.F = \frac{1}{\sqrt{L\,C}} \quad (5)$$

where:

$F = frequency$

L = Main winding synchronous inductance.

C = Capacitance of the capacitor to be connected at main winding.

$$C = \frac{1}{\omega_o^2.L} = \frac{1}{\{(2\pi.F.)^2.L\}} \quad (6)$$

$$C = 23.532\,uF$$

Then, the value of the capacitor to be connected to the main winding (C_{main}) is 23.532 uF. The nearest value for the standard market is 24 uF.

Table 1. Electrical specification of the electric motor pump for this research.

Motor type	Single phase induction motor (fix capacitor starting)
Rated power	250 watt
Working voltage	220 volt
Working frequency	50 Hz
Rotor speed	2950 rpm

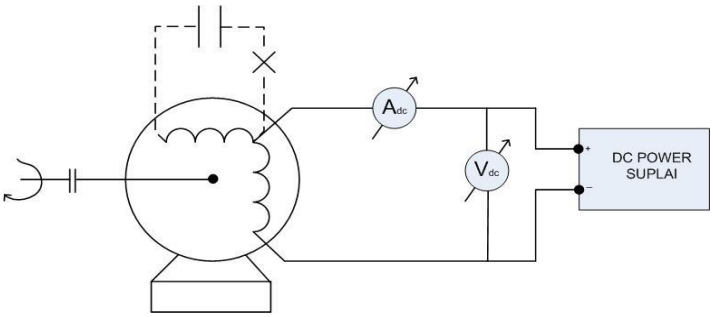

Fig. 6. Winding resistance measuring circuit.

2.3. Collecting dynamic data

The system is a MIMO plant, which consists of two inputs variables and two output variables as shown in Fig. 7. There are six-step to measures the dynamic response of the plant:

- Determining the G_{vv} transfer function by injecting the step signal at the V_{in} point using the I/O port of the USB DAQ board, and measuring the V_{out} output signal for a certain time, while the zero signal is applied to the F_{in} point.
- Determining the G_{ff} transfer function by injecting the step signal at the F_{in} point using the I/O port of the USB DAQ board, and measuring the output signal F_{out} in a specified time, while the zero signal is applied to the V_{in} input.

- Determining the G_{vf} transfer function by injecting the step signal at the V_{in} point using the I/O port of the DAQ USB board, and measuring the F_{out} output signal within a certain time, while the zero signal is applied to the F_{in} input.
- Determining the G_{fv} transfer function by injecting the step signal at the F_{in} point using the I/O port of USB DAQ board, and measuring the output signal V_{out} within a certain time, while a zero signal is applied to V_{in} input.
- Normalizing the voltage and frequency measured data to per unit (p.u.) equivalent value.
- Estimating the transfer function of; G_{vv}, G_{ff}, G_{vf}, and G_{ff} using Identification Toolbox of Matlab base on input-output measured data

The usage of USB DAQ simultaneously acquired V_{out} and F_{out} data, including its time stamps data. The LabView software for data acquisition is shown in Figs. 8 and 9. Figure 8 is the VI diagram, while Fig. 9 is the VI front panel of the software. The acquired data are saved in CSV format or Excel format and then exported to Matlab for further analysis.

Figures 10(a) to (d) are the result of data acquisition as mentioned above. This graph illustrates the input-output responses of blocks G_{vv}, G_{ff}, G_{vf} and G_{fv}. These data are used as a basis for estimating the transfer function of the plant.

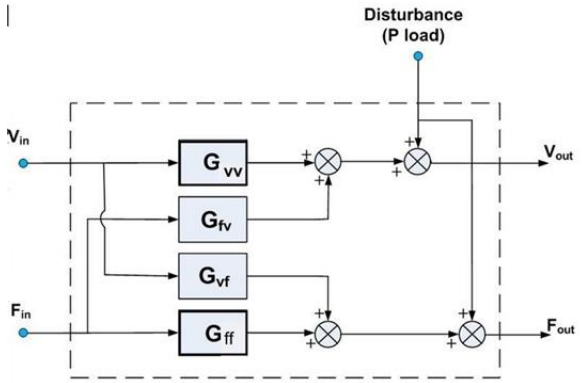

Fig. 7. Plant model block diagram.

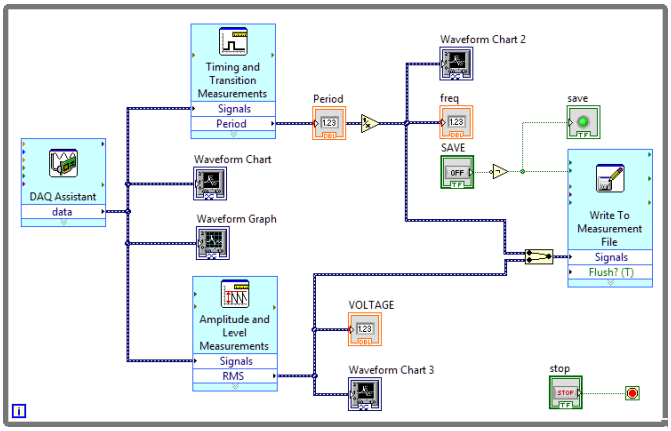

Fig. 8. Labview VI diagram for acquiring voltage and frequency data.

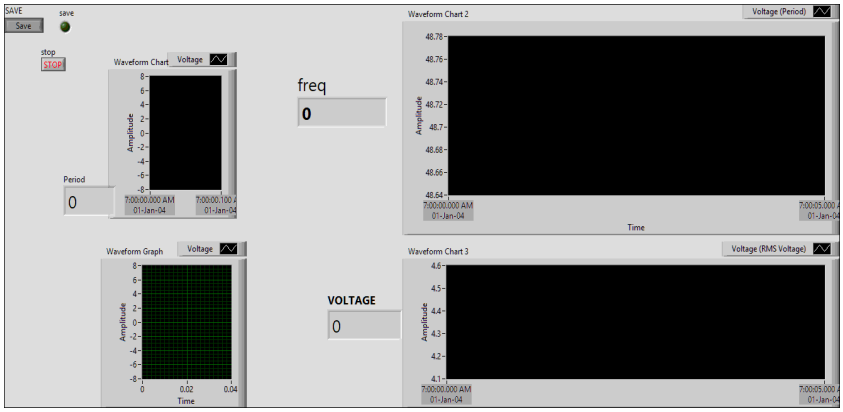

Fig. 9. Labview VI front panel of voltage and frequency data acquisition.

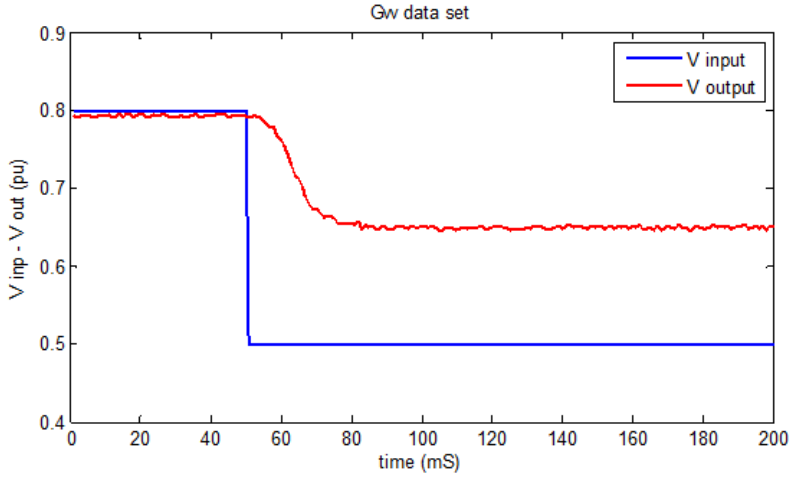

(a) Measured data set for G_{vv}.

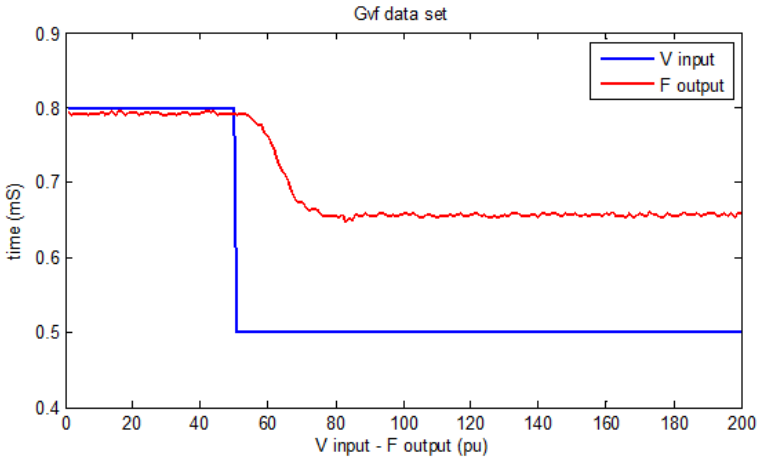

(b) Measured data set for G_{vf}.

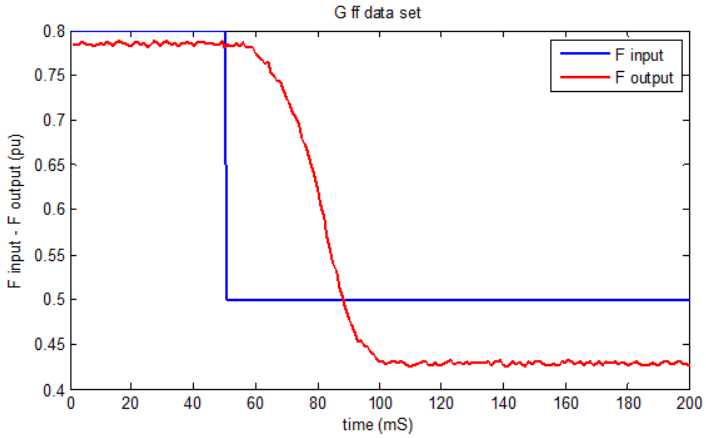

(c) Measured data set for G_{ff}.

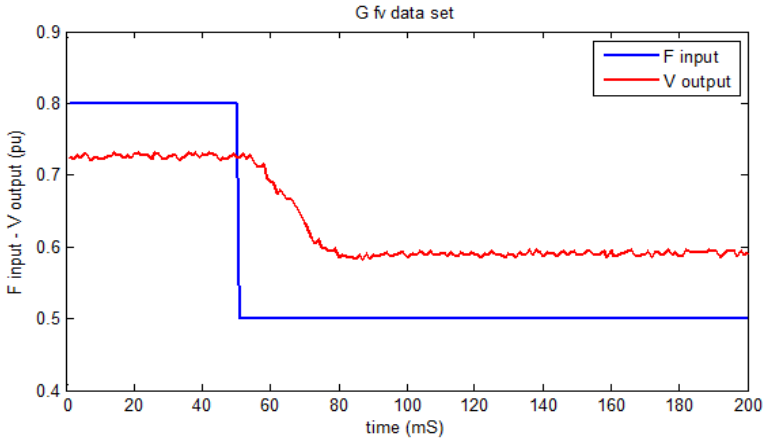

(d) Measured data set for G_{fv}.

Fig. 10. Input-output measured data-set graph of plant for transfer function estimation purposes.

3. Results and Discussion

In this study, the generator output voltage can be controlled by adjusting the position of the binary switch, which serves to connect capacitors to auxiliary winding; while the output frequency can be controlled, by adjusting the electric load balance.

To get a simple and robust control system, the two PID controllers combined with two decouple block can be implemented.

3.1. Estimation of plant dynamic model

There are two approaches that can be used to identify the transfer function of a plant, mathematical approach and "Data-driven" approach. The mathematical approach requires a very complex physical and mathematical calculation of the plant, while the "data-driven" approach requires only the data sets of the input-

output response of the plant. In this study, a "data-driven" approach is used to estimate the transfer function of the plant.

Figure 11 shows the screen shot of the identification toolbox Matlab, which is used to estimate the transfer function of the model under study. Identification process of each block, such as G_{vv}, G_{ff}, G_{vf}, and G_{fv} of the MIMO plant is conducted by using the "Identification toolbox" of Matlab. The necessary data set shows in the Figs. 10(a) to (d) is used as the data input of this GUI. The result of identification is tabulated in Table 2. The block configuration of the MIMO system completed with the transfer-function in Matlab Simulink is shown in Fig. 12.

Table 2. Result of model plant TF estimation using Matlab toolbox.

No.	Block	Estimated transfer function	Percentage fit
1.	G_{vv}	$= \frac{0.2\,s^2 - 1.2\,s + 0.2}{s^3 + 2.13\,s^2 + 2.21\,s + 0.21}$	87.02%
2.	G_{vf}	$= \frac{0.9\,s + 0.87}{s^2 + 2.79\,s + 3.892}$	90.07%
3.	G_{ff}	$= \frac{0.19\,s^2 + 1.21\,s + 0.82}{0.95s^3 + 2.21\,s^2 + 2.32\,s + 0.36}$	91.33%
4.	G_{fv}	$= \frac{0.82\,s + 0.91}{s^2 + 3.11\,s + 4.14}$	98.00%

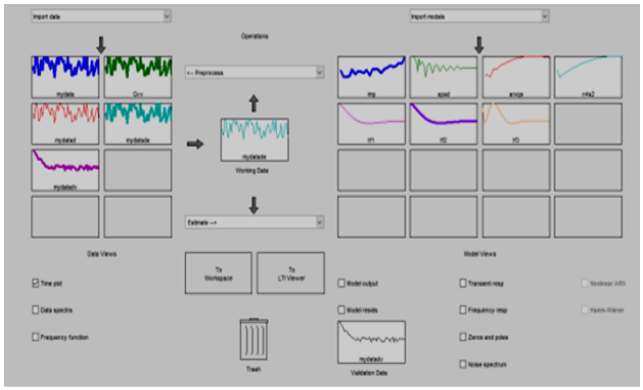

Fig. 11. Identification toolbox Matlab GUI.

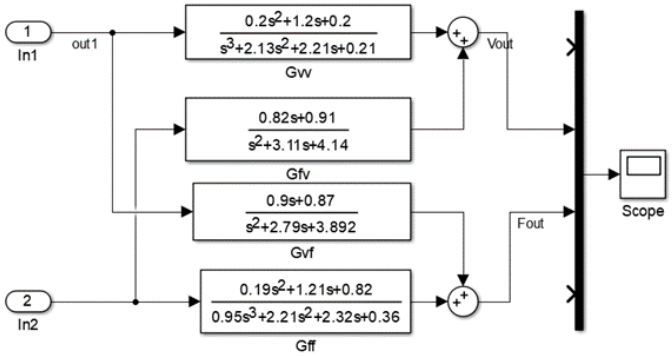

Fig. 12. Transfer function of the plant.

3.2. Matlab simulation

In the MIMO-type plant model, the changes in input value on one loop affected the output value of the other loop. Based on these phenomena the changes of V_{in} input will also cause a change in Fout value. Likewise, a change in F_{in} value also causes a change in V_{out} output (coupling effect). To reduce the coupling effect between these loops, decouple block "*D*" can be added The transfer function of the block decouple (*D*) is:

$$D = \begin{bmatrix} 1 & \frac{-G_{fv}(s)}{G_{vv}(s)} \\ \frac{-G_{fv}(s)}{G_{ff}(s)} & 1 \end{bmatrix} \quad (7)$$

The transfer function of the decouple block "*D*" must have denominator coefficient value which is smaller than the numerator; otherwise, the transfer function must be optimized to get the most optimum coupling reduction effect. Figure 13 shows the transfer function of the plant being study.

Transfer function of the pico-hydro system plant model after being added with decouple block "*D*" is shown in Fig. 14.

The performance of the plant model of this pico-hydro control system, especially the dynamic response of the output voltage and output frequency, can be observed by simulating the transfer function model of the Fig. 14 above by using Matlab Simulink.

In order to obtain a simple and compact control system design, a control system consisting of two PID controllers is used for the voltage loop control and the frequency loop control; two decoupling blocks are added to reduce the coupling effect in-between loops. Practically, decoupling block can be a part of PID controller software embedded in microcontroller hardware or another embedded system. Complete Simulink block diagram to simulate this pico-hydro model is shown in Fig. 15.

The simulation is done by injecting the step voltage signal 0 to 0.5 pu at the input of the voltage set-point and followed by injection the same signal at the input of frequency set-point (the time difference between the two signals is 170 mS). The value of 1.0 pu equals to 250 volts and 50 Hz.

The simulation results are tabulated in Table 3. The auto-tuning facility of PUL Simulink controller obtained PID controller parameters as listed in Table 3. The proportional and integral gain of PID controller loop-1. The proportional and the integral gain value of PID controller no.1 are negative because the opposite gain polarity is needed.

Figure 16 shows the dynamic response from the Matlab Simulink simulation. The blue line is a voltage set-point signal input of the voltage control loop; while the green line is the output voltage of the generator. The cyan line is a frequency set-point signal input for the frequency control loop; while the red line is the output frequency of the generator. From this simulation, it is found that the system is still in a stable condition under changes in voltage set-point or changes in frequency set-point. Changes in the voltage set-point have no significant effect on the output frequency, but changes in the frequency set-point have a significant effect on the output voltage.

Table 3. Setting parameter of PID controllers.

PID loop-1		PID loop-2	
Proportional gain (P)	-0.26618	**Proportional gain (P)**	0.91875
Integral gain (I)	-0.021327	**Integral gain (I)**	1.7251
Derivative gain (D)	0.27658	**Derivative gain (D)**	0

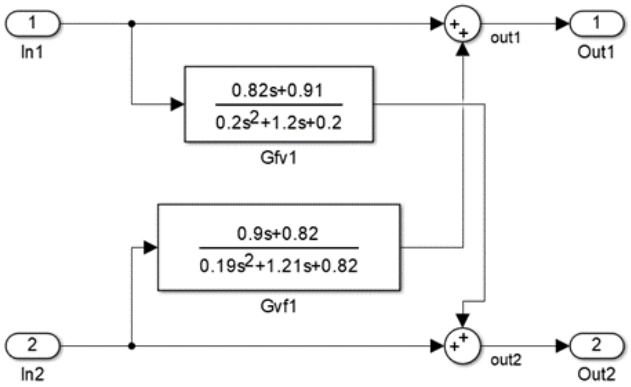

Fig. 13. Decouple circuit block.

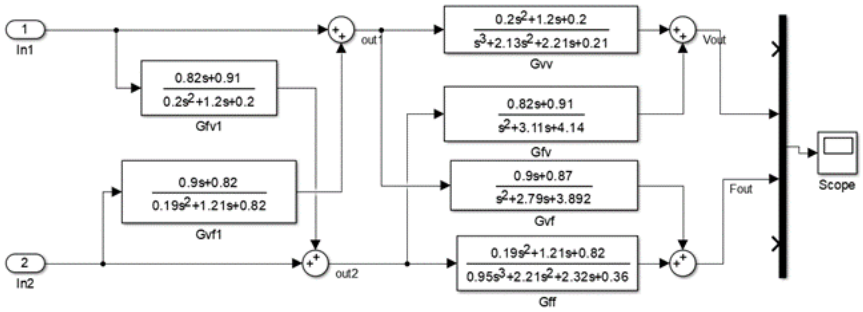

Fig. 14. Plant model completed with decoupling block.

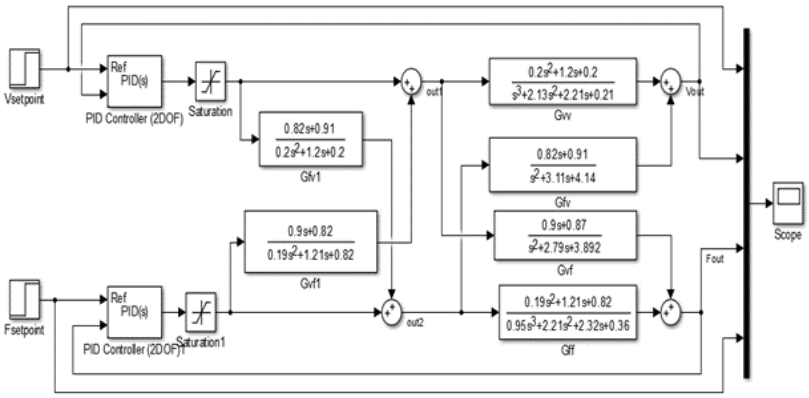

Fig. 15. Matlab Simulink block diagram for performance simulation.

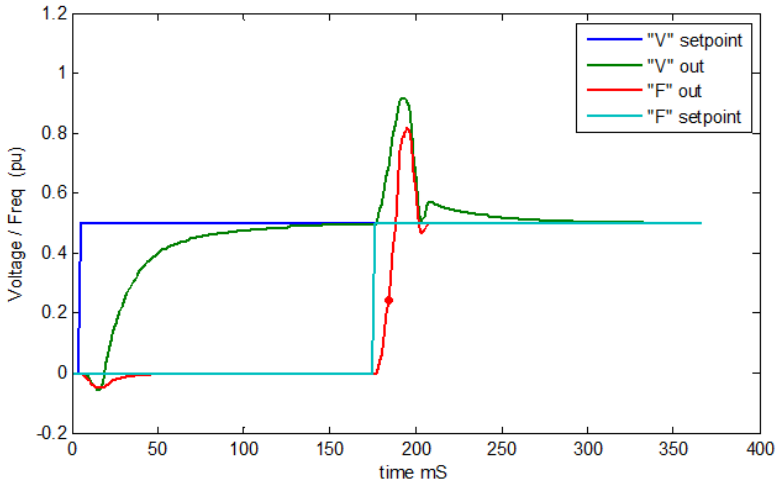

Fig. 16. Simulation result of voltage and frequency response.

4. Conclusions

The rural people have the opportunity to use this idea to produce cheap electrical energy. This is possible because they are familiar with the type of water pump used as the object of this research. It does not take a special engineer or technician to install this simple power plant system. The ease of spare-parts procurement will support long-term system reliability.

The rotor speed controller using the electric balance load method has a good response and cost-effective solution to replace the mechanical speed controller, especially for off-grid pico-hydro scale power plants.

The "data-driven" model-based data estimation method is quite simple and effective to obtain a dynamic model of a system that does not have enough information from the pump manufacturer.

Voltage and frequency regulator using dual PID controllers and the addition of decoupling blocks can significantly reduce output voltage and frequency steady-state errors. From the simulation results obtained, if the frequency-voltage controller is not activated, the 0.3 pu change in the voltage input set-point will produce steady-state error value of output voltage of 0.15 pu; and 0.3 pu change at the frequency input set-point produces steady state error output frequency of 0.08 pu. When the voltage and frequency regulator unit is activated, a 0.5 pu change at the voltage input set-point produces a steady-state error of 0.0025 pu, and a 0.5 pu set-point frequency produces a steady-state error of 0.0014 pu.

Thus, the application of voltage and frequency controller can improve the performance of the generator output voltage and frequency. A single phase electric water pump equipped with a dual PID controller combined with decouple blocks can be used as a pico-hydropower plant for rural areas that have potential water energy.

This simple pico-hydro power plant system is expected to help people generate cheap electricity and increase the electrification ratio of a country, especially in poor or developing countries.

Acknowledgement

The authors are sincerely grateful to the Ministry of Research, Technology, and Higher Education of the Republic of Indonesia for their financial support for this Research by "PDD" project letter no. 073/SP2H/K7/KM/2017.

Nomenclatures

A_{ac}	Alternating current measurement, Amp
A_{dc}	Direct current measurement, Amp
C_{main}	Capacitor connected to main stator winding, uF
D	Decoupling block transfer-function
F	Generator out-put frequency, Hz
F_{in}	Frequency loop set-point input, pu
F_{out}	Frequency loop out-put, pu
G_{ff}	Frequency control loop transfer-function.
G_{fv}	Cross-coupling from frequency loop to voltage loop transfer-function
G_{vf}	Cross- coupling from voltage loop to frequency loop transfer-function
G_{vv}	Voltage control loop transfer-function
L	Main stator winding inductance, Henry
R_{syn}	Main stator winding synchronous resistance, Ohm
V_{ac}	Alternating current voltage measurement, Volt
V_{dc}	Direct current voltage measurement, Volt
X_{syn}	Main stator winding Synchronous Reactance, Ohm
Z_{syn}	Main stator winding Synchronous Impedance, Ohm

Abbreviations

CSV	Comma Separated Value
I/O	Input-Output Port
LSB	Least Significant Bit
MIMO	Multi Input Multi Output
PAT	Pump as Turbine
PID	Proportional Integral Derivative
PVC	Poly Vinyl Chloride
SPSEIG	Single Phase Self Excited Induction Generator
STATCOM	Static Synchronous Compensator
SVC	Static VAR Compensator
USB-DAQ	Universal Serial Bus-Data Acquisition
VI	Virtual Instrument

References

1. Murthy, S.S.; Ahuja, R.K.; Chaudhary, J.K. (2011). Design and fabrication of a low cost analog electronic load controller for a self excited induction generator supplying single-phase loads. *Proceedings of the IEEE International Conference on Power and Energy Systems*. Chenai, India, 1-4.
2. Jain, S.V.; and Patel, R.N. (2014). Investigations on pump running in turbine mode: A review of the state-of-the-art. *Renewable and Sustainable Energy Reviews*, 30, 841-868.

3. Motwani, K.H.; Jain, S.V.; and Patel, R.N. (2013). Cost analysis of pump as turbine for pico hydropower plants - A case study. *Procedia Engineering*, 51, 721-726.
4. Teuteberg, B.H. (2010). Design of a pump-as-turbine microhydro system for an abalone farm. Department of Mechanical and Mechatronic Engineering, Stellenbosch University. *Final Report for Mechanical Project 878*.
5. Derakhshan, S.; and Nourbakhsh, A. (2008). Experimental study of characteristic curves of centrifugal pumps working as turbines in different specific speeds. *Experimental Thermal and Fluid Science*, 32(3), 800-807.
6. Agarwal, T. (2012). Review of pump as turbine (PAT) for micro-hydropower. *International Journal of Emerging Technology and Advanced Engineering*, 2(11), 163-169.
7. Derakhshan, S.; and Nourbakhsh, A. (2008). Theoretical, numerical and experimental investigation of centrifugal pumps in reverse operation. *Experimental Thermal and Fluid Science*, 32(8), 1620-1627.
8. Kusakana, K. *(*2014). A survey of innovative technologies increasing the viability of micro-hydropower as a cost effective rural electrification option in South Africa. *Renewable and Sustainable Energy Reviews*, 37, 370-379.
9. Laghari, J.A.; Mokhlis, H.; Bakar, A.H.A.; and Mohammad, H. (2013). A comprehensive overview of new designs in the hydraulic, electrical equipments and controllers of mini hydro power plants making it cost effective technology. *Renewable and Sustainable Energy Reviews*, 20, 279-293.
10. Ahshan, R.; and Iqbal, M.T. (2009). Voltage controller of a single phase self-excited induction generator. *The Open Renewable Energy Journal*, 2, 84-90.
11. Mossad, M.I. (2011). Control of self excited induction generator using ANN based SVC. *International Journal of Computer Applications*, 23(5), 11-25.
12. Gopal, V.R.; and Singh, B. (2011). Decoupled electronic load controller for offgrid induction generators in small hydro power generation. *International Journal of Emerging Electric Power Systems*, 12(1).
13. Kasal, G.K.; and Singh, B. (2008). Decoupled voltage and frequency controller for isolated asynchronous generators feeding three-phase four-wire loads. *IEEE Transactions on Power Delivery*, 23(2), 966-973.
14. Tiwari, A.K.; Murty, S.S.; Singh, B.; and Shridar, L. (2003). Design-based performance evaluation of two-winding capacitor self-excited single-phase induction generator. *Electric Power Systems Research*, 67(2), 89-97.
15. Chilipi, R.R.; Singh, B.; Murthy, S.S.; Madishetti, S.; and Bhuvaneswari, G. (2014). Design and implementation of dynamic electronic load controller for three-phase self-excited induction generator in remote small-hydro power generation. *IET Renewable Power Generation*, 8(3), 269-280.
16. Chermiti, D.; and Khedher, A. (2014). A new method voltage and frequency regulation of self-excited induction generator operating in stand alone. *WSEAS Transactions on Environment and Development*, 10, 150-159.
17. Said, I.K.; and Pirouti, M. (2009). Neural network-based load balancing and reactive power control by static VAR compensator. *International Journal of Computer and Electrical Engineering*, 1(1), 25-31.
18. Chauhan, Y.K.; Jain, S.K.; and Singh, B. (2012). Performance of self-excited induction generator with cost-effective static compensator. *Maejo International Journal of Science and Technology*, 6(1), 12-27.